Makara Seri Teknologi, 2013, 17(3): In Press
doi: 10.7454/mst.v17i3.xxxx

Surface Modification of Graphite-Encapsulated Iron Compound Magnetic Nanoparticles by Radio Frequency Inductively-Coupled Plasma for Biomolecules Immobilization

Teguh Endah Saraswati[1,2], Akihisa Ogino[1], and Masaaki Nagatsu[1*]

1. Graduate School of Science and Technology, Shizuoka University, 3-5-1, Johoku, Naka-ku, Hamamatsu 432-8561, Japan
2. Department of Chemistry, Faculty of Mathematics and Natural Sciences, Sebelas Maret University, Surakarta 57126, Indonesia

[*]*e-mail: tmnagat@ipc.shizuoka.ac.jp*

Abstract

We proposed the graphite-encapsulated iron compound magnetic nanoparticles as a candidate of nanomaterial due to their potential properties on physical, chemical and biological fields. This study was performed in three steps, starting from the nanoparticle fabrication, nanoparticle surface modification by plasma treatment, leading to biomolecules immobilization for testing the treated nanoparticles capabilities. After the plasma treatment, the surface of the outmost graphene layer is successfully covered by nitrogen-containing groups definitively assigned by XPS spectra and the STEM-EDS elemental mapping. The nitrogen-containing groups formed during the post-treatment plasma selectively attached on the outmost of graphene layer. The inner structure of inner graphene layer and the iron core are still found in stable condition which means that the applied plasma condition allows the efficient covalent functionalization of nitrogen-containing group to the surface particles without give any destruction. The results shows the highest values of N/C atomic ratio of 5.4% is obtained by applying 10 min of Ar plasma pre-treatment and 2 min of NH_3 plasma post-treatment conducted in RF power of 80W and gas pressure of 50 Pa. Finally, in the biomolecules section, it is found that the primary amino groups grafted after Ar plasma pre-treatment followed by NH_3 plasma post-treatment appeared to play an important role in dextran immobilization. The primary amines provide a high selective reaction between aldehyde group of oxidized dextran and amino groups of treated nanoparticles, hence the covalent immobilization was successfully achieved. The dextran immobilization was confirmed by XPS and HR-TEM analysis followed by amino group derivatization using TFBA. The deconvoluted peak at ~398.6 eV (C=N) (as an evidence for Schiff-base linkages between dextran and amino groups on the treated nanoparticles) increased with the increasing of the dextran concentration. This result is consistent with the decrease of free amino group percentage remaining on the nanoparticles surfaces which was evidenced when the dextran concentration increased. High magnification images obtained by HR-TEM allowed the visual observations of the differences between surface morphology of nanoparticles before and after dextran immobilization.

Abstrak

Modifikasi Permukaan pada Nanopartikel Magnetik Senyawa Besi Berlapis Grafit oleh *Inductively-Coupled Plasma* Frekuensi Radio untuk Imobilisasi Biomolekul. Kami mengusulkan agar nanopartikel magnetik senyawa besi berlapis grafit digunakan sebagai nanomaterial karena potensi fisika, kimiawi, dan biologis yang dimilikinya. Penelitian ini dilakukan dalam tiga tahap, yaitu fabrikasi nanopartikel, modifikasi permukaan nanopartikel oleh perlakuan plasma, dan imobilisasi biomolekul untuk menguji kemampuan nanopartikel yang diteliti. Setelah perlakuan plasma dilaksanakan, permukaan lapisan grafena terluar berhasil dilapisi oleh kelompok-kelompok berisi nitrogen, dan hal ini dibuktikan melalui pengujian spektrum XPS dan pemetaan elemen STEM-EDS. Kelompok-kelompok berisi nitrogen yang terbentuk setelah perlakuan plasma diikat secara selektif pada lapisan grafena terluar. Struktur dalam pada lapisan grafena dalam dan inti besi ditemukan dalam kondisi yang masih stabil. Hal ini menunjukkan bahwa fungsionalisasi kovalen yang efisien dan tanpa kerusakan pada kelompok berisi nitrogen terhadap partikel permukaan grafena dapat terjadi karena keadaan plasma yang dikondisikan dalam penelitian. Hasil penelitian menunjukan nilai tertinggi rasio atomik N/C sebesar 5.4% yang diperoleh dari penerapan pra-perlakuan plasma Ar selama 10 menit dan pasca-perlakuan plasma NH_3 selama 2 menit yang dilakukan dengan daya RF sebesar 80 W dan tekanan gas sebesar 50

Pa. Selanjutnya, pada aspek biomolekul ditemukan adanya peran penting yang dipegang oleh kelompok-kelompok amino primer yang ditransplantasi setelah pra-perlakuan plasma Ar, dan pasca-perlakuan plasma NH_3 dalam imobilisasi dekstran. Amino-amino primer memberikan reaksi tingkat tinggi yang selektif antara kelompok aldehida dari dekstran teroksidasi dan kelompok amino dari nanopartikel yang diberikan perlakuan sehingga imobilisasi kovalen dapat tercapai. Imobilisasi dekstran telah dibuktikan oleh analisis XPS dan HR-TEM yang dilanjutkan dengan derivatisasi kelompok amino menggunakan TFBA. Dekonvolusi tertinggi mencapai ±398.6 eV (C=N) (hal ini adalah bukti adanya hubungan basa Schiff antara dekstran dan kelompok amino pada nanopartikel yang diteliti), dan akan meningkat sejalan dengan bertambahnya konsentrasi dekstran. Hasil ini sejalan dengan penurunan persentase sisa kelompok amino bebas pada permukaan nanopartikel yang dibuktikan ketika konsentrasi dekstran meningkat. Gambar dengan magnifikasi tinggi yang dihasilkan oleh HR-TEM menampilkan observasi visual terhadap perbedaan antara morfologi permukaan nanopartikel pada saat sebelum dan sesudah terjadinya imobilisasi dekstran.

Keywords: biomolecule immobilization, magnetic nanoparticles, surface modification

1. Introduction

Iron nanoparticles as magnetic nanoparticles are one of the excellent candidates for biotechnology applications including magnetic resonance (MR) imaging contrast agents, targetable drug carriers, hyperthermia - inducing agents, and magnetically controlled media for the sensitive separation and detection of biomolecules [1-3].

Carbon nanoparticles are as well no less interesting in these applications because they have a large surface area and the ready ability to be functionalized, which make them suitable for high-capacity binding of biomolecules. Using protective shells or coatings on the outside of magnetic nanoparticles such as carbon, organic polymer, or silica, has become an important issue to make them more compatible to bioapplications. Bare magnetic nanoparticles have many limitations such as instability towards oxidation in air, dissolution in acids, and easy agglomeration. At present, graphite-encapsulated magnetic nanoparticles are promising candidate materials in drug delivery application. The carbon or graphite layers can prevent the iron nanoparticles from being rapidly oxidized, and also the carbon layers magnetically isolate the nanoparticles from each other [4].

Among various functional groups for bioapplication, the introduction of amino groups composed of primary amines to the particles surface achieves enhanced wettability and improves its adhesion. Some early work by I.H. Loh, et al. reports the use of ammonia plasma, nitrogen and nitrogen/hydrogen mixtures on carbon black [5]. Recently, there are also several other papers studying about the amino functionalization for carbon nanotubes [6-7], amorphous carbon sheet [8], nanocrystalline diamond [9-10], carbon nanoparticles [11], etc. However, this modification has not been deeply studied on carbon encapsulated magnetic nanoparticles. In fact very few information can be found on the topic of graphite encapsulated iron nanoparticles related to the plasma surface treatment in order to introduce nitrogen-containing group functionalities, such as amino group.

In drug delivery applications, due to the fact that these materials would be used in vivo environments, a fine and homogenous in liquid (usually water) dispersion of the nanoparticles is required. However, the fabricated particles typically contain elemental carbon which is strongly hydrophobic and tends to aggregate when introduced into water. A proper surface modification could enhance the independent dispersion capability and achieve a uniform and stable dispersion. In order to address the issue of particle agglomeration, we propose to modify the nanoparticle surface via plasma processing followed by biomolecules immobilization. Plasma treatment is one of the efficient methods in the field of surface modification. Compared to chemical modification techniques, plasma treatment has the advantages of shorter reaction time, nonpolluting processing, while providing a wide range of different functional groups [12] which might be further used to connect and deliver the therapeutic agents in a biomedical application.

This paper reports about amino groups grafting onto the surface of graphite-encapsulated magnetic iron compound nanoparticles by plasma processing followed by biomolecules immobilization. In detail, this study was performed in three steps, starting from the nanoparticle fabrication, nanoparticle surface modification by plasma treatment, and leading to biomolecules immobilization for testing the treated nanoparticles capabilities. In the first section, the fabrication of nanoparticles by arc discharge method is presented. As a second step, the nanoparticles were treated by radio frequency (RF) inductively-coupled plasma in argon (Ar) and ammonia (NH_3) during two separated stages, aiming to introduce amino functional groups. Lastly, to test the ability of particles to be applied as drug delivery systems, oxidized dextran was immobilized onto the nanoparticles surfaces.

Makara Seri Teknologi, 2013, 17(3): In Press
doi: 10.7454/mst.v17i3.xxxx

2. Experiment

Preparation sample before dextran immobilization: The graphite-encapsulated iron compound nanoparticles were prepared by arc discharge method [13-14]. Following synthesis, the nanoparticles were treated in an inductively-coupled radio frequency plasma device, described in [15]. The chamber diameter and height are both 200 mm each. The water cooling copper pipe helical antenna (100 mm coil diameter, and 20 mm pipe diameter) was coupled to an RF power generator at 13.56 MHz via a matching network. The typical input RF power was about 80 W. The samples were set in a glass dish placed on a stage inside the chamber. There were two steps of the plasma treatment performed in this configuration. First, pretreatment was applied for 10 min using Ar plasma, followed by varied post-treatment 2, 5 and 10 min of NH_3 plasma post-treatment for amino group introduction. During the experiments the gas pressure was varied as 5, 10 and 50 Pa at a fixed gas flow rate of 50 sccm. After plasma treatment, the treated samples were characterized by XPS (Shimadzu ESCA-3400) with Mg Kα X-Ray source and EDS elemental mapping (JEOL, JEM-2100F).

Immobilization of dextran: First, dextran was activated by oxidation with analytical grade reagent - sodium periodate ($NaIO_4$). Different amounts of dextran (0.0625, 0.25, and 0.5 grams to which we shall refer as DX1, DX2, and DX3, respectively) were dissolved in 25 ml pure water. An equal volume of pure water containing 0.625 g of $NaIO_4$ was slowly added and the mixture was stirred at room temperature for 15 hrs in the dark. The oxidized dextran solution was used without further purification. The plasma activated nanoparticles were immersed into the oxidized dextran solutions for 10 hrs, and then washed several times in pure water. As shown in **Error! Reference source not found.**, the amino groups attached to the graphene layer of nanoparticles might react with the aldehyde groups of oxidized dextran forming Schiff-base linkage. To determine the amount of free amino groups on the surface of the nanoparticles, amino group derivatization was carried out using TFBA as reagent. The immobilized nanoparticles were immersed in TFBA solution for 2 hrs then washed in ethanol. Characterization of the nanoparticles was performed before and after immobilization by XPS and HR-TEM.

3. Results and Discussion

To investigate the effect of chemical modification on the plasma-treated surfaces by Ar and NH_3 plasma, XPS measurements were carried out. The relative compositions of C 1s, N 1s, O 1s and Fe 2p, and atomic ratios of O/C and N/C of the samples before and after plasma treatment under different plasma conditions are listed in Table 1.

The experimental results show that the relative composition of C 1s decreased after plasma treatment due to the ion bombardment of Ar plasma pre-treatment. With the Ar plasma pre-treatment, many free carbon bonding are expected to be created in the outmost of graphene layer and then react directly with NH_3 plasma to introduce the amino group on the particle surface.

Comparing to the untreated sample, O/C atomic ratio of the samples after plasma treatment increased. The increase of O/C atomic ratio may be resulted from the following processes. First, carbon radicals are formed in the outermost shell of graphene layers by Ar plasma pre-treatment and NH_3 plasma post-treatment, where the sample surfaces are bombarded by electrons and ions and provide graphene layers with graphite bonding that would be lopped off to form carbon radicals. These radicals then can easily connect with oxygen after opening to the atmosphere, which may result in the increasing of O/C atomic ratio.

The increase of N/C atomic ratio indicates the formation of some nitrogen-containing groups on the outmost of graphene layers by NH_3 plasma treatment. As for the treatment time, in the case of plasma condition at 5 Pa, the post-treatment time does not give a significant influence to the N/C atomic ratio. While the plasma condition at 10 Pa, the increase of post-treatment time will also make an increase their N/C atomic ratio. On the other hand, in the case of plasma condition at 50 Pa, the result is contrary. The highest enrichment of nitrogen-containing functionalities shown from N/C atomic ratio was obtained in the case of 2 min NH_3 plasma post-treatment at 50 Pa. The nitrogen percentage decreased when the period time of post-treatment is longer than 2 min. This indicates that in the case of treatment in 50 Pa, NH_3 plasma post-treatment time

Table 1. Atomic Composition of C 1S, O 1S, N 1S and FE 2P Peaks and Atomic Ratio of O/C and N/C Taken from the XPS Spectra Before and After Plasma Treatment under Various Plasma Conditions

Sample	Treatment period (min)		Atomic composition (%)					Atomic ratio (%)	
	Pre-treatment	Post-treatment	C 1s	O 1s	N 1s	Fe 2p 3/2	Fe 2p 1/2	O/C	N/C
Untreated	–	–	87.91	10.68	0.00	0.82	0.59	12.15	0.00
80 W, 5 Pa	10	2	76.02	19.01	1.15	2.26	1.56	25.01	1.51
	10	5	74.62	18.18	1.11	3.31	2.78	24.36	1.49
	10	10	85.50	11.22	0.94	1.43	0.90	13.12	1.10
80 W, 10 Pa	10	2	81.02	14.72	1.02	2.24	1.01	18.17	1.26
	10	5	80.15	16.05	1.73	1.67	0.40	20.02	2.16
	10	10	76.93	16.12	3.51	1.58	1.87	20.95	4.56
80 W, 50 Pa	10	2	81.30	12.14	4.40	1.75	0.40	14.93	5.41
	10	5	82.13	12.48	1.90	2.44	1.05	15.20	2.31
	10	10	82.91	12.71	1.08	2.19	1.10	15.33	1.30

Plasma condition: Ar and NH_3 gas flow was kept on 50 sccm.

longer than 2 min is too long because the bound amino groups would be released by the electrons and ions existing in NH_3 plasma. On the other hand, it is expected that opposite phenomena occur for plasma treatment performed in 10 Pa. The treatment times of 2 and 5 min at 10 Pa are still not optimum enough for linking nitrogen-containing groups.

The treated sample shown in Fig. 1 corresponds to the treated sample with the highest enrichment of nitrogen-containing groups (80 Watt, 50 Pa, 10 min of pre-treatment and 2 min of post-treatment). There is a significant peak can be observed at around 400.0 eV in the N 1s spectra, which is possibly identified as nitrogen-containing functional group, such as -C–NH_2 at 399.56 eV (L) and other substitutional sp^2 nitrogen in the hexagonal rings of a graphene structure at 400.84 eV (M) [16-18]. The highest atomic percentage of nitrogen is 4.40% increased from 0% of the control sample (untreated).

Beside the XPS spectra, the surface analysis of the treated sample is also carried out by the scanning TEM (STEM) image together with an energy dispersive X-ray spectroscopy (EDS) elemental mapping. After taking the STEM images, the EDS elemental mapping can be performed to address the element composition variation in the area of a STEM image. In Fig. 2, the left image (image in white and black color) represents to a STEM image of the treated sample while the four images in the right hand side represent to the EDS elemental mapping of C, Fe, O and N elements, respectively. For example, the map for C element shows the contrast area at the boundary side of particles which correspond to the graphene layers while the map for Fe element shows the contrast area on the core part of particles which correspond to the iron core nanoparticles. The map of O element has a contrast area in the center of the particle but in less contrast compared to the map of Fe element. It indicates that the oxygen may be mainly found in the iron core nanoparticle rather than on the particle surfaces. On the other hand, the map of N element has a contrast area over the whole area of particles but in less contrast. It indicates that the nitrogen element is found on the whole surface area of the particles, which means that the surface modification successfully attach the nitrogen-containing groups on the outmost of particle surfaces. From the dominant signal at around 399 eV in N 1s region found in XPS spectra, it is considered that they are very likely to be amino group.

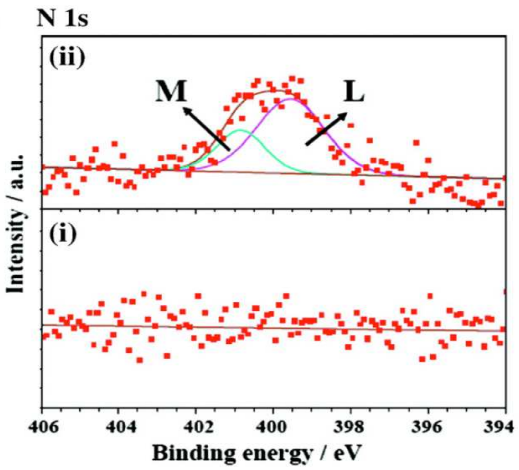

Figure 1. XPS Spectra in N Region Before (i) and After (ii) Plasma Treatment with Condition: 10 min of Ar Plasma Pre-treatment Followed by with 2 min of NH_3 Plasma Post-treatment Performed at 80 W of RF Power and 50 Pa of Gas Pressure

The proposed mechanism of the nitrogen groups attachment is explained as follows: during the plasma exposure, ion bombardment during the pre-treatment by argon plasma provides a sufficient energy to weaken and break the C-C bonds of the outmost of graphene layer, hence allowing the nitrogen-containing groups formed on the surface of graphene layers after post-treatment of NH_3 plasma. The nitrogen-containing groups formed during the post-treatment plasma selectively attached on the outmost of particle surface (graphene layer). Furthermore, the structural of inner graphene layers and the iron core are still found in stable condition. This means that the ammonia plasma allows the efficient covalent functionalization of nitrogen-containing group to the surface particles without giving any destruction. These features are very analogous to the results of amino group addition on the carbon nanotube by ammonia plasma modification [6].

Following plasma treatment, dextran immobilization was achieved. In this step, we applied the best condition found in the previous experiment in a two-stages plasma treatment: 10 min of Ar plasma pre-treatment, and 2 min

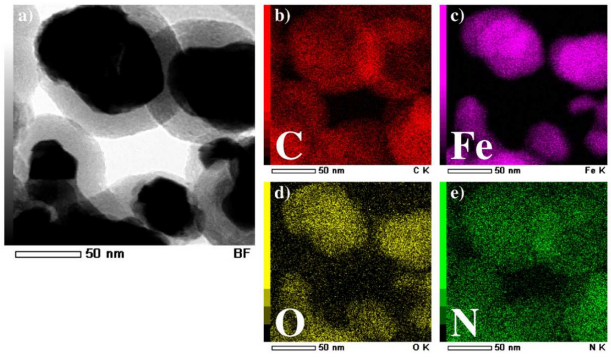

Figure 2. STEM Image (a) and EDS Elemental Mapping Images (b, c, d, and e) of C, Fe, O and N Elements, Respectively, of Treated Sample with Condition: 10 min of Ar Plasma Pretreatment Followed by 2 min of NH_3 Plasma Post-treatment Performed at 80W of RF Power and 50 Pa of Gas Pressure

Makara Seri Teknologi, 2013, 17(3): In Press
doi: 10.7454/mst.v17i3.xxxx

of NH_3 plasma post treatment, both performed using 80 W RF power, and 50 Pa gas pressure. Fig. 3 shows the XPS spectra of the untreated, NH_3 plasma post-treated, and dextran-immobilized nanoparticles in a wide range of binding energies. There are two new peaks in the XPS spectra of DX1 and DX2 around 620-640 eV. These peaks were identified as corresponding to I $3d_{5/2}$ and I $3d_{3/2}$ at 624.8, and 636.2 eV, respectively, originating from the excess of $NaIO_4$ [19-20]. In contrast, these peaks do not appear in the spectrum of DX3 immobilized nanoparticles. The absence of peaks at the binding energy corresponding to I 3d shows that there was no excess $NaIO_4$ in the DX3 solution, therefore all the $NaIO_4$ molecules were used to oxidize the dextran in the solution with the higher dextran concentration, DX3 (20% solution).

After plasma treatment, the C 1s core peak intensity decreased, probably because during the pre-treatment, Ar plasma might have broken carbon double bonds in the graphene structure. Ar plasma successfully created dangling bonds and reactive radicals to form aminated surfaces in the latter plasma post-treatment step, or oxidized-surfaces (due to reaction with oxygen from atmospheric air). The latter phenomenon can explain the increasing of the intensity of O1s peak after plasma treatment. Some references also mention that Ar plasma might play a role in surface contamination removal and increase of surface roughness for better adhesion [21].

After immobilization, the intensity of C1s state peak increased due to the carbon contained by dextran molecules. In Fig. 3, it is shown that the intensity of C1s peak significantly increased with increasing the dextran concentration. The intensity of C1s peak of DX3 is higher than DX2 which is higher than DX1. Similar to C1s, the intensity of O1s peak was found to increase with increasing the dextran concentration. It is well known that dextran have many oxygen atoms, and gets more oxygen atoms after oxidation by sodium periodate. The oxygen in $NaIO_4$ might also contribute to the increase in the O1s peak, especially in DX1 and DX2 spectra.

The concentration of amino group can be estimated from the concentration of fluorine of TFBA molecules from amino group derivatization. The number of fluorine atom corresponds to the number of amino groups according to the derivatization protocol. Based on reaction between primary amino group and TFBA [6,22], the percentage of free amino groups can be estimated from the equation below:

$$\%NH_2 = \left[\frac{NH_2}{N}\right] = \frac{([F]/3)}{[N]} \times 100\%$$

Using the equation above, we can calculate the percentage of amino groups attached onto the nanoparticle surface as being 68.09±5.10%, 63.68±4.72%, 38.71±5.81%, and 14.73±5.89% for treated, DX1, DX2, and DX3 immobilized nanoparticles, respectively. The error bar is estimated from the signal-to-noise ratio of F1s XPS spectra. The decrease of free amino groups percentage with increasing the concentration of dextran solution indicates that more amino group have been used to form covalent bonds with aldehyde groups of dextran. In other words, it can be concluded that more dextran is immobilized onto the nanoparticles, as in the case of DX3, as the concentration of dextran solution increases. This result has a good agreement with the increasing of deconvoluted C=N peak in the N 1s XPS. The relation between the percentage of C=N bonds and the percentage of free amino groups is presented in Fig. 4. It shows that the increasing of the number of C=N bonds corresponds to the decreasing of the percentage of free amino groups remaining onto the surface of nanoparticles.

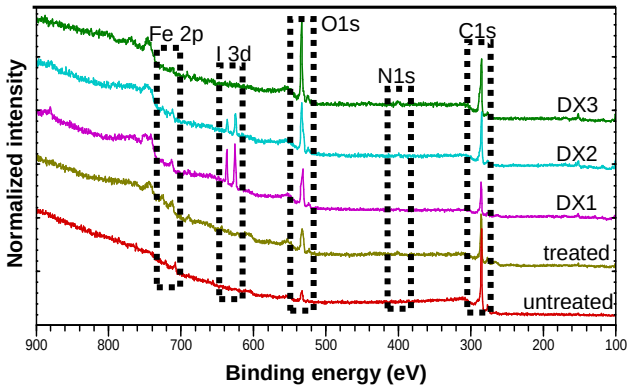

Figure 3. Wide XPS Spectra of Untreated, Treated, and Immobilized DX1, DX2, and DX3 Nanoparticles. The Spectra were Taken Before Performing Amino Group Derivatization

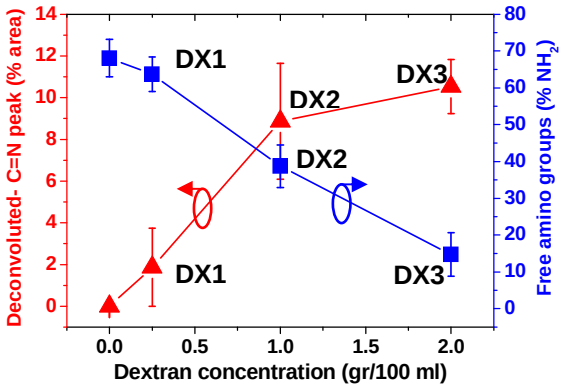

Figure 4. The Dependence of Area Percentage of C=N Peak Taken from N1s XPS Spectra Before Amino Group Derivatization and Atomic Percentage Free Amino Groups Estimated by Chemical Derivatization vs. Dextran Concentration. Error Bars Represent Uncertainty in Determining Peak Intensities in the Peak Fitting Procedure

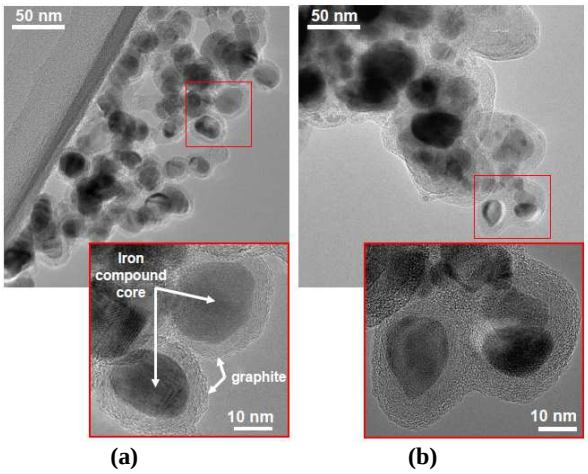

Figure 5. Magnified TEM Images of Untreated (a), and Dextran Immobilized (b) Nanoparticles

To confirm the immobilization of biomolecules, we carried out HR-TEM observations of the nanoparticles which have immobilized dextran on the surfaces. Typical HR-TEM images of untreated and plasma treated samples are shown in Fig. 5. The dextran immobilized nanoparticles were found in large packed agglomerates. Compared with the surface morphology of the untreated and treated nanoparticles, HR-TEM images clearly show the structural surface modification especially observed on the surface of the nanoparticles. After the dextran immobilization, the slightly thicker non-crystalline layer covering the particle surface was additionally formed shown in the inset image in Fig. 5 (right image). This fact might be due to the coating of dextran and adsorption of water or organic molecules from atmospheric air. The coating of dextran represents some large organic molecules which contain mostly carbon and oxygen and have no visible lattice fringes. Therefore, the existence of dextran molecules surrounding the nanoparticles surface caused the difficulty in analyzing the graphite layers under TEM observation.

4. Conclusions

After the plasma treatment with experimental condition applied here, the surface of the outmost graphene layer is successfully covered by nitrogen-containing groups definitively assigned by XPS spectra and the STEM-EDS elemental mapping. The nitrogen-containing groups formed during the post-treatment plasma selectively attached on the outmost of graphene layer. The inner structure of inner graphene layer and the iron core are still found in stable condition which means that the applied plasma condition allows the efficient covalent functionalization of nitrogen-containing group to the surface particles without give any destruction.

After biomolecules immobilization, the dextran immobilization was confirmed by XPS and HR-TEM analysis followed by amino group derivatization using TFBA. The deconvoluted peak at ~398.6 eV (C=N) (as an evidence for Schiff-base linkages between dextran and amino groups on the treated nanoparticles) increased with the increasing of the dextran concentration. This result is consistent with the decrease of free amino group percentage remaining on the nanoparticles surfaces which was evidenced when the dextran concentration increased. High magnification images obtained by HR-TEM allowed the visual observations of the differences between surface morphology of nanoparticles before and after dextran immobilization.

Acknowledgment

This work was supported in part by a Grants-in-Aid for Scientific Research (Grant No. 2110010) from the Japan Society for the Promotion of Science (JSPS).

References

[1] C.C. Berry, J. Phys. D: Appl. Phys. 42 (2009) 224003.
[2] Q.A. Pankhurst, N.K.T. Thanh, S.K. Jones, J. Dobson, J. Phys. D: Appl. Phys. 42 (2009) 224001.
[3] G. Pastorin, Pharm. Res. 26 (2009) 746.
[4] M. Bystrzejewski, A. Huczko, H. Lange, Sens. Actuators B: Chem. 109 (2005) 81.
[5] I.H. Loh, R.E. Cohen, R.F. Baddour, J. Mater. Sci. 22 (1987) 2937.
[6] C. Chen, B. Liang, D. Lu, A. Ogino, X. Wang, M. Nagatsu, Carbon 48 (2010) 939.
[7] A. Felten, C. Bittencourt, J.J. Pireaux, G. van Lier, J.C. Charlier, J. Appl. Phys. 98 (2005) 074308.
[8] N. Inagaki, K. Narushima, H. Hashimoto, K. Tamura, Carbon 45 (2007) 797.
[9] Z. Remes, A. Choukourov, J. Stuchlik, J. Potmesil, M. Vanecek, Diamond Relat. Mater. 15 (2006) 745.
[10] Z. Remes, A. Kromka, M. Vanecek, A. Grinevich, H. Hartmannova, S. Kmoch, Diamond Relat. Mater. 16 (2007) 671.
[11] W.-K. Oh, H. Yoon, J. Jang, Diamond Relat. Mater. 18 (2009) 1316.
[12] C.L. Chen, A. Ogino, X.K. Wang, M. Nagatsu, Appl. Phys. Lett. 96 (2010) 3.
[13] M. Nagatsu, T. Yoshida, M. Mesko, A. Ogino, T. Matsuda, T. Tanaka, H. Tatsuoka, K. Murakami, Carbon 44 (2006) 3336.
[14] Y. Saito, T.Yoshikawa, M.Okuda, N.Fujimoto, S.Yamamuro, K.Wakoh, K.Sumiyama, K. Suzuki, A. Kasuya, Y. Nishina, Chem. Phys. Lett. 212 (1993) 379.

Makara Seri Teknologi, 2013, 17(3): In Press
doi: 10.7454/mst.v17i3.xxxx

[15] T.E. Saraswati, T. Matsuda, A. Ogino, M. Nagatsu, Diam. Relat. Mat. 20 (2011) 359.
[16] G. Beamson, D. Briggs, High Resolution XPS of Organic Polymers: The Scienta ESCA 300 Database, John Wiley & Sons, Chichester, 1992, p.280.
[17] K. Schroder, B. Finke, A. Ohl, In: R. D'Agostino, P. Favia, C. Oehr, M.R. Wertheimer, (Eds.), Plasma Processes and Polymers: 16th International Symposium on Plasma Chemistry Taormina, Italy June 22-27, 2003, Wiley InterScience, Weinheim, 2005, p.545.
[18] S. Point, T. Minea, B. Bouchet-Fabre, A. Granier, G. Turban, Diamond Relat. Mater. 14 (2005) 891.
[19] P.M.A. Sherwood, J. Chem. Soc. Faraday Trans. 2: Mol. Chem. Phys. 72 (1976) 1805.
[20] M.J. van Stipdonk, V. Santiago, E.A. Schweikert, C.C. Chusuei, D.W. Goodman, Int. J. Mass Spectrom. 197 (2000) 149.
[21] A. Ogino, S. Noguchi, M. Nagatsu, J. Photopolym Sci. Technol. 22 (2009) 461.
[22] I. Losito, E. de Giglio, N. Cioffi, C. Malitesta, J. Mater. Chem. 11 (2001) 1812.